J Radioanal Nucl Chem (2013) 298:1215–1220
DOI 10.1007/s10967-013-2593-9

Preparation and biological distribution of ^{99m}Tc-cefazolin complex, a novel agent for detecting sites of infection

M. El-Tawoosy

Received: 6 February 2013 / Published online: 2 July 2013

Abstract The optimization of the radiolabeling yield of cefazolin with ^{99m}Tc was described. Dependence of the labeling yield of ^{99m}Tc-cefazolin complex on the amounts of cefazolin and $SnCl_2{\cdot}2H_2O$, pH and reaction time was studied. Cefazolin was labeled with ^{99m}Tc with a labeling yield of 89.5 % by using 1 mg cefazolin, 5 μg $SnCl_2{\cdot}2H_2O$ at pH 4 and 30 min reaction time. The radiochemical purity of ^{99m}Tc-cefazolin was evaluated with ITLC. The formed ^{99m}Tc-cefazolin complex was stable for a time up to 3 h, after that the labeling yield decreased 64.0 % at 8 h. Biological distribution of ^{99m}Tc-cefazolin complex was investigated in experimentally induced inflammation mice, in the left thigh, using *Staphylococcus aureus* (bacterial infection model) and turpentine oil (sterile inflammation model). Both thighs of the mice were dissected and counted and the ratio of bacterial infected thigh/contralateral thigh was then evaluated. In case of bacterial infection, T/NT for ^{99m}Tc-cefazolin complex was 8.57 ± 0.4 after 0.5 h, which was higher than that of the commercially available ^{99m}Tc-ciprofloxacin under the same experimental conditions. The ability of ^{99m}Tc-cefazolin to differentiate between septic and aseptic inflammation indicates that ^{99m}Tc-cefazolin could undergo further clinical trials to be used for imaging sites of infection.

Keywords Cefazolin · Ciprofloxacin · ^{99m}Tc · Infection · Inflammation

M. El-Tawoosy (✉)
Labeled Compound Department, Hot Lab Centre, Atomic Energy Authority, P.O. Box 13759, Cairo, Egypt
e-mail: m_eltawoosy@yahoo.com

Introduction

Bacterial infection is a major problem worldwide, and especially in the developing countries. Many a time these processes result in significant patient morbidity, permanent disability or even death [1]. Infections, especially internal infections, resulting in delayed diagnosis, treatment, and sometimes death, were difficult to detect in the early stages. Several imaging methods like ultrasonography (US), computer tomography (CT) and magnetic resonance imaging (MRI) are available and have been used for the past several decades for the localization of infection. But it is well known that these are not the best of methods for the localization of infection at early stages. These procedures detect the morphologic alterations of the tissues after significant process has taken place in the infective process leading to abscess formation [2]. Nuclear medical imaging has an important role in discriminating infections from inflammations. Inflammatory processes can be visualized in their early phases, when anatomical changes are not yet apparent since scintigraphic images are based on functional changes of tissues. In this connection, various radiopharmaceuticals, such as radiolabeled antimicrobial peptides and antibiotics have been developed [3–5]. The early detection of the infectious focus by radionuclide imaging helps both patient and physician and reduces the time and cost of treatment. The radiopharmaceuticals routinely used for scintigraphic detection include ^{67}Ga-citrate [6], ^{99m}Tc or ^{111}In-labeled leukocytes [7], ^{99m}Tc-nano-colloid [8], ^{99m}Tc or ^{111}In-labeled HIG (human polyclonal immunoglobulin) [9, 10] and ^{99m}Tc-ubiquicidin-29-41 [11–13].

On the other hand, a non-specific ^{99m}Tc-human immunoglobulin (HIG) [14] and liposomes [15, 16] accumulate at an infection/inflammatory site without distinction between bacterial infection and non-bacterial inflammation. The

mechanism of non-specific localization is facilitated by locally enhanced vascular permeability [14]. Recently, several radiopharmaceuticals have been developed to differentiate between infection and sterile inflammation [17–20]. However, none of these are infection specific because sensitivity and specificity can differ according to the type of micro-organism, infection, infection site and clinical conditions/response. Clearly, radiopharmaceuticals that bind to a variety of bacteria would be better candidates for specific infection imaging [21]. The first to be proposed was ciprofloxacin radiolabeled with ^{99m}Tc, which is supposed to bind to DNA-gyrase and topoisomerase IV of bacteria, as does unlabeled ciprofloxacin [22]. However, previously reported data about the specificity of ^{99m}Tc-ciprofloxacin for infection are contradictory [20, 23–28]. ^{99m}Tc-ciprofloxacin preparation has some disadvantages related to radiochemical purity (81 ± 4 %) [29] and stability which are discussed in details in the literature [1, 2, 29–31]. So other antimicrobial agents such as levofloxacin [32], pefloxacin [33], lomefloxacin [20], norfloxacine [34], cefoprazone [35], sparafloxacin [36], cefuroxime [37], Novobiocin [38], ceftriaxone [39] and HQMADA [40] were labeled with ^{99m}Tc to be used for imaging sites of infection and to overcome the drawback of ^{99m}Tc-ciprofloxacin.

Cefazolin is one of cephalosporin antibiotics. It is mainly used to treat bacterial infections of the skin. It can also be used to treat moderately severe bacterial infections involving the lung, bone, joint, stomach, blood, heart valve, and urinary tract. It is clinically effective against infections caused by staphylococci and streptococci of Gram-positive bacteria. These organisms are common on normal human skin.

This work aims to study the labeling conditions and biological distribution of ^{99m}Tc-cefazolin in inflammation bearing animals.

Experimental

Cefazolin was purchased from Pharco B international company, Alex., Egypt and all other chemicals were purchased from Merck and they were reactive grade.

Preparation of stock solution of $SnCl_2 \cdot 2H_2O$

Exactly weighed 190 mg of stannous chloride dihydrate was completely dissolved in 0.5 ml Conc. HCl by heating on a hot plate then the volume was completed to 10 ml using nitrogen purged double distilled water. Each ml contains 19 mg of stannous chloride equivalent to 10 mg of tin (II). One ml was again diluted to 100 ml with nitrogen purged double distilled water. Two ml of this solution was dispensed in a 10 ml clean penicillin vial, flushed with nitrogen gas for 15 min, then stored at ≈ −20 °C for future use. The final concentration was 0.1 mg tin/ml (84.2×10^{-5} mol).

Labeling procedure

Accurately weighed 1 mg cefazolin was transferred to a penicillin vial then the vial was evacuated. Exactly 50 µl of $SnCl_2 \cdot 2H_2O$ stock solution (5 µg Sn) was added, then the volume of the mixture was completed to one ml by N_2-purged distilled water. One ml of freshly eluted $^{99m}TcO_4^-$ (400 MBq) was added to the above mixture. The reaction mixture was vigorously shaken and allowed to react at room temperature for sufficient time required to complete the reaction.

Analysis

The labeling yield and radiochemical purity were determined by thin layer chromatography. The reaction product was spotted on silica gel ITLC-SG strips (Sigma Chemical Company, USA) (10×1.5 cm^2 sheets) and developed in acetone and saline as the mobile phase. After developing, they were cut into 1 cm pieces and counted.

Free $^{99m}TcO_4^-$ in the preparation was determined using acetone as the mobile phase. Reduced hydrolyzed technetium was determined by using saline as the mobile phase.

It was further confirmed by a Shimadzu HPLC system, which consists of pumps LC-9A, UV spectrophotometric detector operated at a 230 nm (SPD-6A), and rheodyne injection valve. Chromatographic analysis of ^{99m}Tc-cefazolin was performed by injection of 10 µl of the reaction mixture at the optimum conditions into a reversed-phase column (RP-C18; 5 µm, 4 mm × 250 mm, Lichrosorb) and the column was eluted with mobile phase consisting of acetonitrile and water (43:57 *v/v*), and the flow rate was adjusted to 1 ml/min. The mobile phase was filtered and degassed prior to use. Fractions of 1 ml were collected separately using a fraction collector up to 14 ml and assayed in a well-type NaI(Tl) detector connected to a single-channel analyzer.

Biological evaluation

The study was approved by the animal ethics committee, Labeled Compounds Department and was in accordance with the guidelines set out by the Egyptian Atomic Energy Authority. Biodistribution of ^{99m}Tc-cefazolin was evaluated in male Swiss mice (body mass 30–40 g). To induce the inflammation, autoclaved turpentine oil, approximately 10^7–10^8 colony forming units of *Staphylococcus aureus* suspended in 0.2 ml of saline were administrated into the

left thigh. For quantitative determination of organ distribution, five mice were used for each experiment and 0.1 ml of about 18 MBq of ^{99m}Tc-complex solution was injected into the tail vein of mice after 24 h of bacterial induction. Then the mice were sacrificed by the decapitation under chloroform anesthesia at 1/2, 1 and 2 h post-injection. Blood sample was collected at the time of decapitation. Both thighs (left thigh muscle as target and right thigh muscle as control) and organs were dissected, weighed and their radioactivity was measured using a well-type NaI(Tl) detector connected with a single channel γ-counter (SR-7). Results were expressed as percent of the injected dose per organ or body fluid. Target and non-target thigh radioactivity ratio was also determined. Differences in the data were evaluated with the Student *t* test. Results for *P* using the 2-tailed test are reported and all results are given as mean ± SEM. The level of significance was set at $P < 0.05$.

Results and discussion

Radiochemical purity and stability of ^{99m}Tc-cefazolin complex was assessed by thin layer chromatographic method using acetone as the solvent (about 15–30 min required for developing solvent). Free pertechnetate moves with the solvent front ($R_f = 1$), while ^{99m}Tc-cefazolin complex and reduced hydrolyzed technetium remain at the origin. Reduced hydrolyzed technetium was determined by using saline as the mobile phase (about 30–45 min required for developing solvent), where reduced hydrolyzed technetium remains at the origin ($R_f = 0$) while other species migrate with the solvent front ($R_f = 1$). The radiochemical purity was determined by subtracting the sum of the percent of reduced hydrolyzed technetium and free pertechnetate from 100 %. The radiochemical yield is the mean value of three experiments.

On the other hand, the HPLC purification method was presented in Fig. 1 and showed two peaks, one at fraction No. 3, which corresponds to $^{99m}TcO_4^-$, while the second peak was collected at fraction No. 6, which corresponds to ^{99m}Tc-cefazolin, which was found to coincide with the UV signal. Nearly, 98 % of the injected activity in the HPLC was recovered as collected activity.

The chemical structure of cefazolin is presented in Fig. 2. The various complexes of ^{99m}Tc may be formed by interactions between electron donor atoms and reduced technetium. In order to form bonds with technetium, the structure must contain electron donors such as oxygen, nitrogen and sulfur. Although the exact complex structure is not known, all cephalosporines coordinated with ^{99m}Tc due to the existence of electron donor atoms in their structure [41–44].

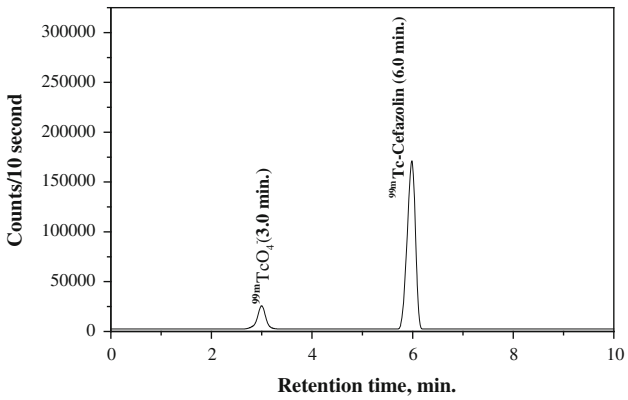

Fig. 1 HPLC radiochromatogram of ^{99m}Tc-cefazolin

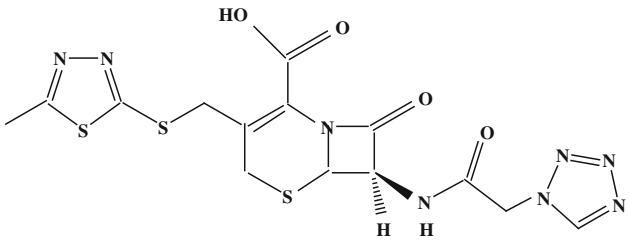

Fig. 2 Chemical structure of cefazolin

Effect of reaction time Figure 3 describes the effect of incubation time on the radiochemical purity of ^{99m}Tc-cefazolin complex. After 1-min post labeling, the yield was low and equals to 41.8 % which increased with time till reaching a maximum value of 89.5 % after 30 min. The yield remains stable at ~86 % for a time up to 3 h after that the yield decreased to reach 64 % after 8 h.

Effect of cefazolin amount The labeling yield of ^{99m}Tc-cefazolin complex increased with increasing the amount of cefazolin. The labeling yield was 39 % using 100 μg cefazolin then reached the maximum value of 89.5 % using 1 mg cefazolin; after that, the formed complex remained

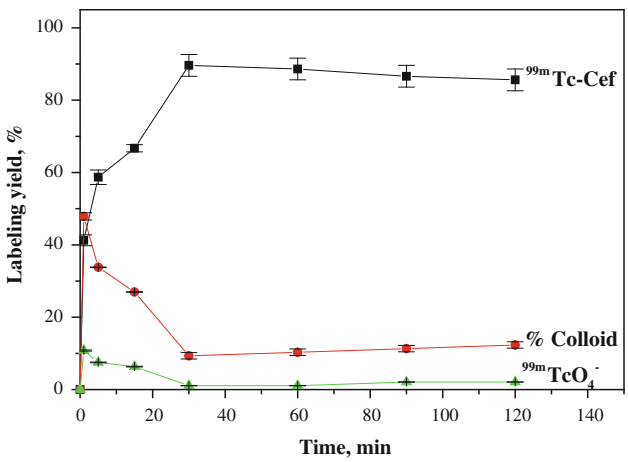

Fig. 3 ^{99m}Tc-cefazolin yields versus reaction time

stable with increasing the amount of cefazolin up to 2 mg. So, the optimum amount of cefazolin was 1 mg (Fig. 4). This is due to the fact that at low cefazolin amount, $SnCl_2{\cdot}2H_2O$ is greater than that of cefazolin, and is easily converted to colloid as the percentage of colloid was 55 % using 100 μg cefazolin.

Effect of $SnCl_2{\cdot}2H_2O$ amount As shown in Fig. 5, the radiochemical yield was dependent on the amount of $SnCl_2{\cdot}2H_2O$ present in the reaction mixture. At 1 μg $SnCl_2{\cdot}2H_2O$, the labeling yield of ^{99m}Tc-cefazolin was 59.8 % due to the fact that $SnCl_2{\cdot}2H_2O$ amount was insufficient to reduce all pertechnetate so the percentage of $^{99m}TcO_4^-$ was relatively high (22.4 %). The labeling yield significantly increased by increasing the amount of $SnCl_2{\cdot}2H_2O$ from 2 to 5 μg (optimum content), at which a maximum labeling yield of 89.5 % was obtained. By increasing the amount of $SnCl_2{\cdot}2H_2O$ above the optimum concentration value, the labeling yield decreased again because excess $SnCl_2{\cdot}2H_2O$ was converted to colloid (44.2 % at 50 μg $SnCl_2{\cdot}2H_2O$).

Effect of pH of the reaction mixture As shown in Fig. 6, the optimum labeling yield was obtained at pH 4 (89.5 %). At higher and lower pH values, the labeling yield was low where at pH 3 the labeling yield of ^{99m}Tc-cefazolin complex was 38.5 % and at pH 11 was 27 %.

Biodistribution

The uptake of the ^{99m}Tc-cefazolin complex in different organs of the animals infected with turpentine oil and *S. aureus* was given in Tables 1 and 2, respectively. ^{99m}Tc-cefazolin was removed from the circulation mainly through the urinary pathway (~38.5 % injected dose after 2 h post injection of the tracer). In the turpentine oil inflamed muscle, a significant large amount of ^{99m}Tc-cefazolin activity was observed in the liver (12.3 %) after 30 min post injection. After 2 h of tracer administration, the major part of activity of ^{99m}Tc-cefazolin was found in the liver (7.92 ± 0.16 %), Kidney (16.88 ± 0.3 %) and intestine (38.17 ± 0.19 %) as shown in Table 1. In contrast, in *S. aureus* inflamed muscle, the liver uptake decreased markedly with time from 10.12 % after 30 min till reaching 7.42 % after 2 h as shown in Table 2. The uptake of ^{99m}Tc-cefazolin was significantly low in turpentine oil infected group of animals (aseptic inflammation) as compared to infected group with living bacteria (abscess). These data indicate rapid distribution throughout the body and uptake in the inflamed areas was observed within 30 min after intravenous injection of the tracer.

As shown in Fig. 7, mice with infectious lesions injected with ^{99m}Tc-cefazolin showed a mean abscess-to-muscle (target-to-non target, T/NT) ratio equals to 8.6 ± 0.4 %, after 30 min post injection. At all time intervals, ^{99m}Tc-cefazolin shows higher T/NT in the infected muscle

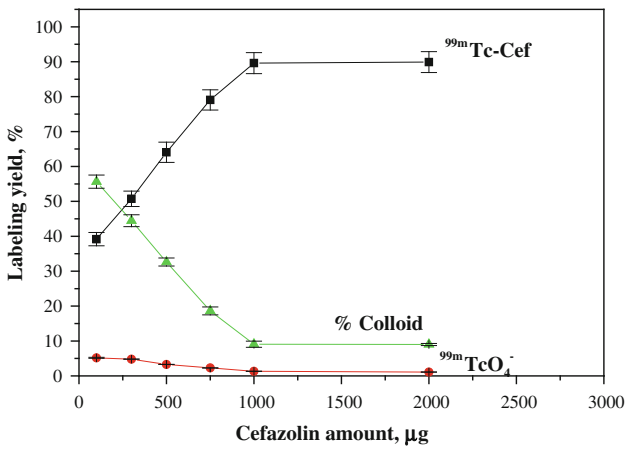

Fig. 4 Percent labeling yield of ^{99m}Tc-cefazolin as a function of substrate concentration

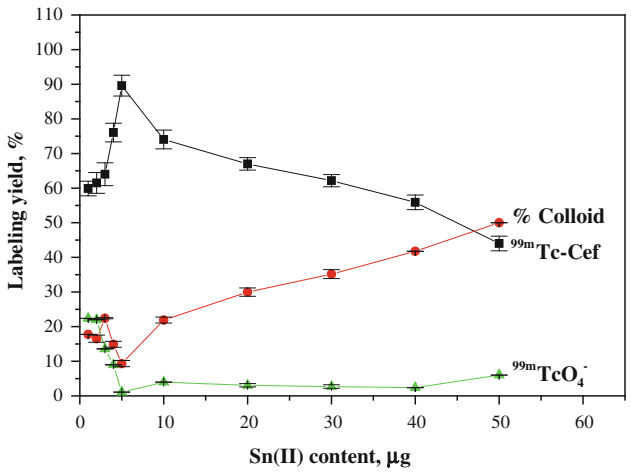

Fig. 5 Effect of $SnCl_2{\cdot}2H_2O$ concentration on the labeling yield of ^{99m}Tc-cefazolin

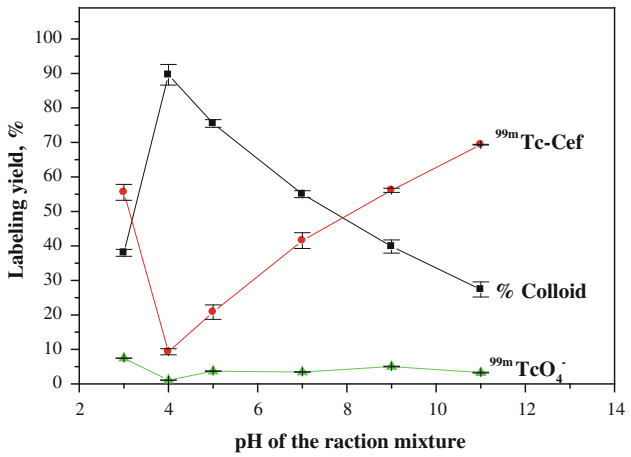

Fig. 6 Effect of pH on the labeling yield of ^{99m}Tc-cefazolin

Table 1 Biodistribution of ^{99m}Tc-cefazolin in turpentine oil inflamed mice at different time intervals

Organs and body fluids	Percent I.D./gram organ		
	Time post injection (min)		
	30	60	120
Blood	1.97 ± 1.10	1.02 ± 0.002*	0.96 ± 0.04*
Bone	0.08 ± 0.01	0.10 ± 0.01*	0.18 ± 0.01*
Control muscle	0.25 ± 0.01	0.10 ± 0.02*	0.09 ± 0.002
Infected muscle	1.23 ± 0.01	0.30 ± 0.02*	0.18 ± 0.01
Liver	12.30 ± 0.05	9.73 ± 0.15*	7.92 ± 0.16*
Urine	16.55 ± 0.07	19.75 ± 0.25	21.25 ± 0.15
Kidney	13.96 ± 0.40	15.01 ± 0.60	16.88 ± 0.30*
Lung	1.20 ± 0.10	0.91 ± 0.12*	0.63 ± 0.02*
Heart	1.05 ± 0.05	0.50 ± 0.05*	0.25 ± 0.01*
Stomach	2.80 ± 0.09	3.51 ± 0.30	2.38 ± 0.16*
Intestine	42.41 ± 0.50	40.24 ± 0.30	38.17 ± 0.19*
Spleen	0.77 ± 0.02	0.56 ± 0.04*	0.34 ± 0.02
T/NT	4.92 ± 0.20	2.98 ± 0.12	2.00 ± 0.10

Values represent mean ± SEM. $n = 6$

* Significantly different from previous value of each organ using unpaired Student's t test ($P < 0.05$)

Table 2 Biodistribution of ^{99m}Tc-cefazolin in *Staphylococcus aureus* inflamed mice at different time intervals

Organs and body fluids	Percent I.D./gram organ		
	Time post injection (min)		
	30	60	120
Blood	1.95 ± 0.10	0.31 ± 0.02*	0.75 ± 0.04*
Bone	0.11 ± 0.02	0.04 ± 0.01*	0.06 ± 0.005*
Control muscle	0.33 ± 0.01	0.86 ± 0.02*	0.03 ± 0.001
Infected muscle	2.83 ± 0.10	5.09 ± 0.02*	0.13 ± 0.10
Liver	10.12 ± 0.15	9.20 ± 0.15*	7.42 ± 0.16*
Urine	16.55 ± 0.07	17.15 ± 0.25	18.45 ± 0.15
Kidney	14.84 ± 0.40	15.10 ± 0.30	20.06 ± 0.60*
Lung	1.99 ± 0.10	0.93 ± 0.12*	1.13 ± 0.20*
Heart	0.85 ± 0.05	0.58 ± 0.05*	0.07 ± 0.01*
Stomach	4.38 ± 0.40	1.91 ± 0.20	1.77 ± 0.16*
Intestine	28.00 ± 0.50	30.01 ± 0.30	31.17 ± 0.70*
Spleen	1.78 ± 0.12	0.61 ± 0.04*	0.67 ± 0.02
T/NT	8.57 ± 0.40	5.91 ± 0.32	4.60 ± 0.21

Values represent mean ± SEM. $n = 6$

* Significantly different from previous value of each organ using unpaired Student's t test ($P < 0.05$)

(*S. aureus*) than in the sterile inflamed muscle (turpentine), so, the use of ^{99m}Tc-cefazolin complex can differentiate bacterial infection from sterile inflammation.

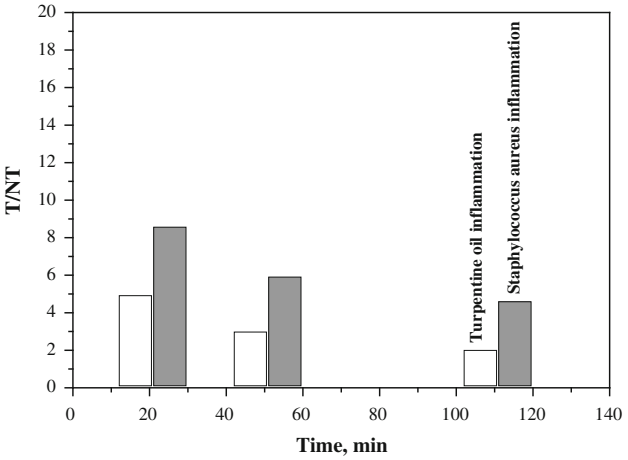

Fig. 7 The ratio of target muscle (T) to non target muscle (NT) of ^{99m}Tc-cefazolin in different inflammation models at different post injection times

As a result, ^{99m}Tc-cefazolin showed higher uptake in infected tissue than the commercially available ^{99m}Tc-ciprofloxacin (T/NT = 3.6 ± 0.4 %) [29]. The mean abscess-to-muscle (T/NT) ratio for ^{99m}Tc-cefazolin was higher than that of other recently published ^{99m}Tc-labeled antibiotics such as sparafloxacin (T/NT = 5.9 ± 0.7 %) [36], difloxacin (T/NT = 5.5 ± 0.5 %) [45], norfloxacin (T/NT = 6.9 ± 0.4 %) [46], rifampicin (T/NT = 7.3 ± 0.7 %) [47], ceftraixone (T/NT = 5.6 ± 0.6 %) [39], streptomycin (T/NT = 2.4 ± 0.1 %) [48], and *N*-sulfanilamide (T/NT = 2.9 ± 0.1 %) [49].

Conclusions

Cefazolin can be labeled easily with technetium-99m using stannous chloride as a reducing agent and gives higher labeling yield (89.5 %) than the commercially available ^{99m}Tc-ciprofloxacin. Biodistribution study for ^{99m}Tc-cefazolin in infected mice demonstrated high and rapid accumulation of ^{99m}Tc-cefazolin at the site of infection compared with ^{99m}Tc-ciprofloxacin. The use of ^{99m}Tc-cefazolin distinguishes infection from sterile inflammation. ^{99m}Tc-cefazolin shows higher mean abscess-to-muscle (target-to-non target, T/NT) ratio in the infected muscle (*S. aureus*) at all time intervals than that of sterile inflamed muscle (turpentine). ^{99m}Tc-cefazolin complex showed higher labeling yield, stability and uptake in infected tissue (T/NT = 8.57 ± 0.4 %) than the commercially available ^{99m}Tc-ciprofloxacin (T/NT = 3.6 ± 0.4 %). These results were promising enough to state that ^{99m}Tc-cefazolin could be used instead of the commercially available ^{99m}Tc-ciprofloxacin as a good radiotracer for imaging of infection at early stages and distinguishing infection from sterile inflammation.

Acknowledgments This work was made by the generous and encouragement of the staff of Radioisotopes Production Division, Hot Laboratories Center, Atomic Energy Authority, Cairo-Egypt. The author would like to thank the referees and the Editor of the Journal of Radioanalytical and Nuclear Chemistry for their valuable notices. Many thanks to Prof. K. Farah for her review and advices.

References

1. Lima JET, Maliska C, Goncalves MRB, Lima RC, Corbo R (2004) World J Nucl Med 3:284
2. Britton KE, Vinjamuri S, Hall AV (1997) Eur J Nucl Med 24:553–555
3. Rennen HJM, Boerman OC, Oyen WJG, Corstens FHM (2004) Med Chem Rev 1:27–30
4. Das SS, Hall AV, Wareham DDW, Britton KE (2002) Braz Arch Biol Technol 45:25
5. Lupetti A, Welling MM, Paulwels EKJ, Nibbering PH (2003) Lancet Infect Dis 3:223–226
6. Seabold JE, Palestro CJ, Brown ML (1997) J Nucl Med 38:994–997
7. Seabold JE, Forstrom LA, Schauwecher DS (1997) J Nucl Med 38:997–999
8. Schrijver MD, Streule K, Senekowitsch R (1987) Nucl Med Commun 8:895–897
9. Buscombe JR, Miller RF, Lui D (1991) Nucl Med Commun 12:583–587
10. McAfee JG, Gagne G, Subramanian G (1991) J Nucl Med 32:2126
11. Akhtar MS, Qaisar A, Irfanullah J (2005) J Nucl Med 46:567–568
12. Akhtar MS, Iqbal J, Khan MA (2004) J Nucl Med 45:849–851
13. Nibbering PH, Welling MM, Paulusma-Annema A (2004) J Nucl Med 45:321–325
14. Rennen HJ, Boerman OC, Oyen WJ, Corstens FH (2001) Eur J Nucl Med 28:241–244
15. Boerman OC, Laverman P, Oyen WJ, Corstens FH, Storm G (2000) Prog Lipid Res 39:461–463
16. Erdogan S, Ozer AY, Ercan MT, Hincal AA (2000) J Microencapsul 17:459–461
17. Singh AK, Verma J, Bhatnagar A, Ali AW (2003) J Nucl Med 2:103–106
18. Martin-Comin J, Soroa V, Rabiller G, Galli R, Cuesta L, Roca M (2004) Rev Esp Med Nucl 23:357–358
19. Gomes Barreto V, Rabiller G, Iglesias F, Soroa V, Tubau F, Roca M (2005) Rev Esp Med Nucl 24:312–315
20. Motaleb MA (2007) J Radioanal Nucl Chem 272:95–97
21. Welling MM, Paulusma-Annema A, Balter HS, Pauwels EKJ, Nibbering PH (2000) Eur J Nucl Med 27:292
22. Fournier B, Zhao X, Lu T, Drlica K, Hooper DC (2000) Antimicrob Agents Chemother 44:2160
23. Sonmezoglu K, Sonmezoglu M, Halac M (2001) J Nucl Med 42:567
24. Yapar Z, Kibar M, Yapar AF, Togrul E, Kayaselcuk U (2001) Eur J Nucl Med 28:822–825
25. Larikka MJ, Ahonen AK, Niemela O (2002) Nucl Med Commun 23:167–169
26. Dumarey N, Blocklet D, Appelboom T, Tant L, Schoutens A (2002) Eur J Nucl Med 29:530–535
27. Welling MM, Lupetti A, Balter HS (2001) J Nucl Med 42:788–790
28. Sarda L, Saleh-Mghir A, Peker C, Meulemans A, Cremieux AC, Leguludec D (2002) J Nucl Med 43:239–240
29. Rien HS, Huub JR, OTTO CB, Rudi D, Guido S (2004) J Nucl Med 42:2088–2090
30. Seung JO, Jin SR, Joong WS, Eun JY, Hyun JH (2002) Appl Radiat Isot 57:193–195
31. Sarda L, Cremieux AC, Lebellec Y, Meulemans A, Lebtahi R (2003) J Nucl Med 44:920–925
32. El-Ghany EA, Amine AM, El-Kawy OA, Amin M (2007) J Label Compd Radiopharm 50:25–29
33. El-Ghany EA, El-Kolaly MT, Amine AM, El-Sayed AS, Abdel-Gelil F (2005) J Radioanal Nucl Chem 266:131–135
34. Ibrahim IT, Motaleb MA, Attalah KM (2010) J Radioanal Nucl Chem 285(3):431–436
35. Motaleb MA (2007) J Radioanal Nucl Chem 272:167–171
36. Motaleb MA (2009) J Label Compd Radiopharm 52:415–418
37. Yurt Lambrecht F, Durkan K, Unak P (2008) J Radioanal Nucl Chem 275:161–166
38. Shah SQ, Khan MR, Khan AU (2011) Radiochim Acta 99:53–58
39. Mostafa M, Motaleb MA, Sakr TM (2010) Appl Radiat Isot 68:1959–1963
40. Motaleb MA, Alabdullah ES, Zaghary WA (2011) J Radioanal Nucl Chem 287:61–67
41. Barreto VG, Iglesias F, Roca M, Tubau F, Martin Comin J (2000) Rev Esp Med Nucl 19:479
42. Roohi S, Mushtaq A, Jehangir M, Malik SA (2006) J Radioanal Nucl Chem 267:561
43. Vallee F, Lebel M (1991) J Antimicrob Agents Chemother 35:2057
44. Mirshojaei SF, Gandomkar M, Najafi R, Sadat Ebrahimi SE, Babaei MH, Shafiei A, Talebi MH (2011) J Radioanal Nucl Chem 287:21–25
45. Motaleb MA (2010) J Label Compd Radiopharm 53:104–109
46. Ibrahim IT, Motaleb MA, Attalah KM (2010) J Label Compd Radiopharm 50:25–29
47. Shah SQ, Khan AU, Khan MR (2010) Appl Radiat Isot 68:2255–2260
48. Meral T, Erean T, Isil SU (1992) J Nucl Med Biol 19:802–806
49. Imen E, Wafa G, Nadia MS, Mouldi S (2010) J Nucl Med Biol 37:821–829